Effect of a Layered Environment on the Complex Natural Frequencies of Two-Dimensional WGM Dielectric-Ring Resonators

Svetlana V. Boriskina, *Member, IEEE*, Trevor M. Benson, *Senior Member, IEEE*, Phillip Sewell, *Member, IEEE*, and Alexander I. Nosich, *Senior Member, IEEE*

***Abstract*—An efficient and accurate algorithm based on the combination of the Green's function method and an analytical regularization technique is applied to study the complex natural frequencies and Q factors of two-dimensional (2-D) dielectric resonators (DRs) in a layered environment. Frequency shift and degeneracy splitting of the whispering-gallery modes (WGMs) of circular-cylindrical and tubular DRs immersed into layered dielectric media are computed and analyzed.**

***Index Terms*—Analytical regularization, dielectric resonators (DRs), Green's functions, optical waveguide components.**

I. Introduction

LOW-LOSS dielectric resonators (DRs) operating on the whispering-gallery modes (WGMs) have been studied both theoretically and experimentally for a number of years. Their various advantages, such as high Q factors, simplicity of fabrication, mechanical stability, good temperature compensation, and suppression of spurious modes promote their widespread use in various optical, microwave and millimeter-wave circuits. Furthermore, they have proven to be essential components for the design of novel optical devices, such as microlasers [1], high-Q wavelength selective filters, wavelength division multiplexers (WDMs) [2], polarization rotators [3], and can be useful for the study of nonlinear optical effects [4].

Knowledge of the natural frequencies and quality factors of *isolated* DRs is of interest for some remote sensing and antenna applications. Indeed, a number of approaches to the investigation of isolated resonators can be found, such as dielectric waveguide methods [5], radial and axial mode-matching methods [6], [7], the method of moments (MoM) [8], the null-field method [9], and finite difference time domain (FDTD) methods [10], [11]. However, in most practical optoelectronic applications, DRs are integrated as a part of a complex circuit. In this case, the natural frequencies can differ significantly from that of an isolated resonator due to field interactions in the coupling region. Accurate prediction of the behavior of such in situ DRs is crucial for full exploitation of their potential, and yet, to date, there is a lack of computationally efficient analysis techniques reported in the literature for this problem.

The objective of this paper is to present such a technique that is not only highly accurate and very fast but also offers flexibility and robustness, essential ingredients for practical design software. Before describing the present approach, a brief review will be made of the existing techniques that have yielded some insight into the performance of such in situ DRs.

Some attempts have been made to study the complex frequencies of DRs in a shielded microwave integrated circuit (MIC) environment and to estimate the degradation of Q factors due to conductor loss. For example, a perturbation method was proposed in [12] for indirect determination of conductor Q factors of DRs by computing the relative difference between the perturbed and unperturbed resonant frequencies. However, it is required that these are evaluated beforehand using a rigorous method. In [13], the conductor Q factor of a DR was determined by computing the stored energy and energy loss by the effective dielectric constant method. Moreover, an accurate technique based on a new definition of effective dielectric constants in the dielectric waveguide model was used in [14] to obtain the resonant frequencies of DRs in MIC environment. The mode-matching technique was applied in [15] to calculate the resonant frequencies of a ring DR on a dielectric substrate and two coupled ring DRs inside a perfectly conducting waveguide cavity.

The analyses just described are only applicable in the shielded case, which is common in microwave applications. However, the study of DR characteristics in a nonshielded and, furthermore, a stratified dielectric environment is much more important for the optoelectronic applications. Unfortunately, this is even more difficult since it requires taking into account the conditions at infinity as well as the continuity conditions at all the dielectric interfaces.

In [16], a simple circuit model of a DR coupled to a transmission line was proposed, and some applications of WGM DRs as bandstop or directional filters and power combiners were discussed. However, the results presented for filter characteristics were mostly experimental. Moreover, in the theoretical treatment, the authors assumed that the radiation losses were almost negligible, which is a very rough approximation for an open system such as a waveguide-coupled DR.

Surface integral equations (IEs) were applied in [17] to study the resonance frequencies of a dielectric disk on a dielectric sub-

Manuscript received April 1, 2002. This work was supported in part by the Royal Society & NATO Postdoctoral Fellowship to S. V. Boriskina.

S. V. Boriskina, T. M. Benson, and P. Sewell are with the School of Electrical and Electronic Engineering, University of Nottingham, University Park, Nottingham NG7 2RD, U.K. (e-mail: eezsb@ gwmail.nottingham.ac.uk).

A. I. Nosich is with the Institute of Radio-Physics and Electronics, National Academy of Sciences of Ukraine, Kharkov, 61085, Ukraine (e-mail: alex@ emt.kharkov.ua).

Digital Object Identifier 10.1109/JLT.2002.800297

strate, although the effect of the substrate-guided waves was neglected. This omission is significant since, in practical situations, it is vital to consider the excitation of resonators by surface waves propagating along dielectric guides or, as in the case of add/drop filters, launching surface waves in different guides by the WGM of a DR. Indeed, as shall be highlighted, the interaction between DRs and dielectric waveguides, along with the radiation losses from the DR, has a dramatic effect on the natural frequencies and especially on Q factors.

A combination of the volume IE method and Galerkin technique was also used to analyze DRs in inhomogeneous environments [18] but is only applicable to resonators with separable geometries, which is too restrictive in practice. The design of waveguide-coupled microring resonators has been performed using FDTD in [19]. However, the computational intensity of FDTD techniques, as well as the need to use high-quality artificial absorbers and to avoid meshing-induced staircasing errors, are well known. Finally, it should also be noted that standard perturbation techniques can fail to give a correct description of the high-Q WGM resonances as the inhomogeneity of the host media causes a drastic shift of the resonant frequencies from their free-space values.

Having discussed the approaches to the problem of in situ DRs considered to date, it is clear that there is a need for a more robust technique, one more suited to modern-day design tasks. Such a technique has been developed in [20] and [21] and successfully applied to study the performance of microwave WGM filters based on the circular and ring DRs excited by a guided mode of a grounded dielectric waveguide. However, the analysis presented in [21] only investigated the scattering problem and as such was formulated entirely in the real-frequency domain. Furthermore, the applications considered in [21] are more suitable for microwave structures.

This paper presents the analysis of the 2-D source-free generalized-eigenvalue problem for a WGM DR in a layered medium. As known, due to a power leakage, open resonators may have only complex-valued natural frequencies that necessitate the analytic continuation of the characteristic eigenvalue problem to the complex domain. The spectrum of complex-valued frequencies does not depend on the DR excitation; hence, their identification is an important task in the practical design process.

There are a number of significant issues that must be resolved when the approach of [21] is generalized to the eigenvalue problems. These include the accurate computation of the Bessel and Hankel functions of complex arguments and numerical treatment of certain integrals not arising in the real-frequency case. Finally, the problem is reduced to searching for the determinantal zeros, which can now occur over a wide range of a complex plane, rather than the real-axis problem previously considered. Therefore, a formulation of the open-DR eigenvalue problem needs special attention, and this is presented in Section II. Section III deals with the derivation of IEs, while Section IV contains a brief description of how a regularized infinite-matrix equation is obtained. Section V contains a review of the major physical effects of the layered host medium on the behavior of natural frequencies. Conclusions are summarized in Section VI. Throughout the paper, the time-dependence convention $e^{-i\omega t}$ is adopted and omitted.

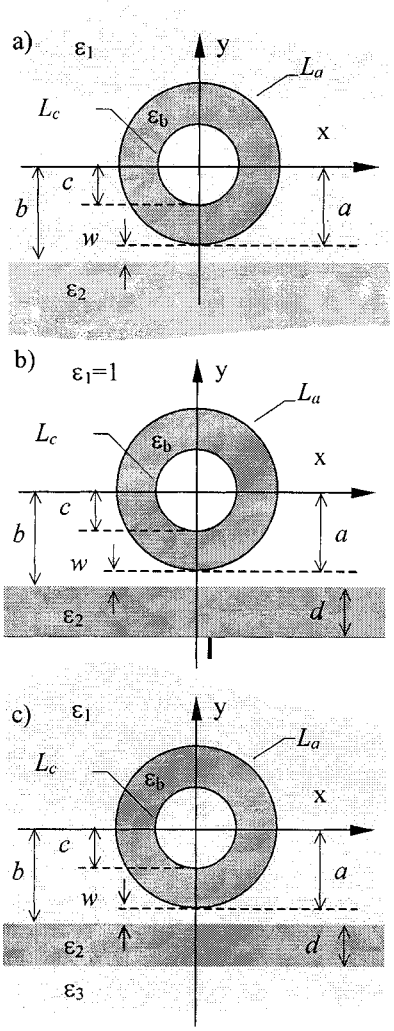

Fig. 1. WGM ring-like DR in stratified media.

II. Eigenvalue Problem Formulation

In many practical optoelectronic applications, DRs are located in the vicinity of flat dielectric interfaces, e.g., semiconductor substrates or planar waveguides. Thus, we consider a tubular dielectric cylinder (ring DR, for brevity) in a layered-dielectric host medium. In particular, we shall consider a pair of dielectric half-spaces [Fig. 1(a)], grounded dielectric slab [Fig. 1(b)] and planar asymmetrical dielectric slab [Fig. 1(c)]. These geometries are of interest for optical bandstop filters, couplers and sensors, and their microwave and millimeter-wave counterparts. The outer and inner radii of the ring are denoted as a and c, respectively. The cylinder separation from the nearest dielectric interface is w, so that the DR center is at distance $b = a + w$ from the interface. We assume a 2-D problem (i.e., that the fields do not vary along the z axis). Then a total field can be characterized by a single scalar function U, which represents either the E_z or H_z component, depending on the polarization. Off the boundaries, the total field must satisfy the Helmholtz equation

$$\left[\Delta + k^2 \varepsilon(\vec{r})\right] U(\vec{r}) = 0 \tag{1}$$

where the permittivity $\varepsilon(\vec{r})$ is, for definiteness, a positive step-wise function of coordinates. Continuity conditions on the circular contours L_a, L_c and at the flat interfaces between the flat layers of the host medium are the same as in the scattering problem (see [21]).

As we consider an open-domain problem, the correct condition should be imposed at infinity in the plane (x, y) for the complex values of k. This condition can be established by using a technique of [22], i.e., by analyzing the far-zone behavior of the layered-medium Green's function analytically continued to complex k. The fields can be represented as convolutions with the Green's functions (see [23]); therefore, they must have the same far-zone behavior. In [22], such a radiation condition was established for the real-k scattering by a localized object in layered medium. It differs from classical Sommerfeld's condition by the presence of the guided-wave modes of host medium. Reichardt's condition [24] is known to be the complex-k continuation of Sommerfeld's condition to the sheets of $\mathrm{Ln}\, k$. In similar manner, in our problem, the following modified condition should be imposed (see Appendix I):

$$U(\vec{r}) \underset{r\to\infty}{\cong} R_j(\vec{r}) + W(\vec{r}), \quad j = 1,2,3$$

$$R_{1,3}(\vec{r}) = \sum_{n=-\infty}^{\infty} \alpha_{(1,3)n}^{E(H)} H_n^{(1)}\left(k\sqrt{\varepsilon_{1,3}}r\right) e^{in\varphi}, \quad R_2(\vec{r}) = 0$$

$$W(\vec{r}) = \sum_{p=1}^{Q^{E(H)}} \left\{ \begin{matrix} \beta_{+p}^{E(H)}, x > 0 \\ \beta_{-p}^{E(H)}, x < 0 \end{matrix} \right\} V_p^{E(H)}(g_p y) e^{ih_p k|x|}. \quad (2)$$

Here, $g_p = \sqrt{\varepsilon_1 - h_p^2}$, $h_p = h_p(k)$, $p = 1, 2, \ldots$ are normalized propagation constants of the natural modes of the host medium, $Q^{E(H)}$ (depends on k) is a number of these modes, and $V_p(g_p y)$ is a mode cross-sectional field (see [21]). Note that $R_3(\vec{r}) = 0$ in the case of Fig. 1(b). Besides, $W(\vec{r}) = 0$ 1) in the case of Fig. 1(a), (2) if $\varepsilon_2 < \varepsilon_1$ in the case of Fig. 1(b), and (3) if $\varepsilon_2 < \max(\varepsilon_1, \varepsilon_3)$ in Fig. 1(c). Coefficients α_{jn} and β_p are some functions of $\mathrm{Ln}\, k$ and $g_p(k)$, and $H_n^{(1)}(\cdot)$ are the Hankel functions. Equation (1), along with the boundary and far-field conditions, defines a generalized eigenvalue problem. As seen from (2), the domain of analytic continuation of the field function in k is not wider than the infinite-sheet Riemann surface Ω of the function $\mathrm{Ln}\, k + \sum_{p=1}^{Q^{E(H)}} (\varepsilon_1 - h_p^2(k))^{1/2}$. On its principal sheet Ω_0, defined by the conditions $-\pi/2 < \arg k < 3\pi/2$ and $\mathrm{Im}(\varepsilon_1 - h_p^2(k))^{1/2} > 0$, $p = 1, 2, \ldots Q^{E(H)}$, the generalized eigenvalues can be located only on the $\mathrm{Im}\ k < 0$ half-plane, coming in pairs symmetric with respect to the imaginary axis.

These facts can be verified by using the complex Poynting theorem applied to the modal field function (i.e., generalized eigenfunction). Note that, at the real axis of Ω_0, condition (2) reduces to the radiation condition established in [22].

III. Boundary Integral Equations (IEs)

Now, we build a coupled set of IEs for the eigenvalue problem formulated in Section II. In doing so, we retrace all the steps of the scattering-problem IEs derivation (see [21]), but keep in mind that now the parameter k can be complex-valued. First, we present the fields outside the outer radius of DR, inside the ring, and inside the inner radius of DR, respectively, as the single-layer surface potentials over the corresponding-domain contour

$$U(\vec{r}) = \int_{L_a} \psi^{E(H)}(\vec{r}_a) G^{E(H)}(\vec{r}, \vec{r}_a) dl_a, \quad r > a \quad (3)$$

$$U^{\mathrm{res}}(\vec{r}) = \int_{L_a} \varphi^{E(H)}(\vec{r}_a) G_\varepsilon^{E(H)}(\vec{r}, \vec{r}_a) dl_a + \int_{L_c} \mu^{E(H)}(\vec{r}_c) G_\varepsilon^{E(H)}(\vec{r}, \vec{r}_c) dl_c, \quad c < r < a \quad (4)$$

$$U^{in}(\vec{r}) = \int_{L_c} \beta^{E(H)}(\vec{r}_c) G_1^{E(H)}(\vec{r}, \vec{r}_c) dl_c, \quad r < c. \quad (5)$$

Validity of representations (3)–(5) for complex k follows from the Reichardt condition (see Appendix I and [23]). Here, $G_\varepsilon^{E(H)}$ and $G_1^{E(H)}$ are the $E(H)$-type Green's functions of the homogeneous medium with permittivity ε_b and ε_1, respectively, and $G^{E(H)}$ is the Green's function of the layered dielectric medium, all continued to complex k, i.e.,

$$G_\varepsilon^{E(H)}(\vec{r}, \vec{r}_a) = \frac{i\alpha}{4} H_0^{(1)}\left(k\sqrt{\varepsilon_b}\,|\vec{r} - \vec{r}_a|\right) \quad (6)$$

$$G_1^{E(H)}(\vec{r}, \vec{r}_c) = \frac{i\alpha}{4} H_0^{(1)}\left(k\sqrt{\varepsilon_1}\,|\vec{r} - \vec{r}_c|\right) \quad (7)$$

$$G^{E(H)}(\vec{r}, \vec{r}_a) = \frac{i\alpha}{4} H_0^{(1)}\left(k\sqrt{\varepsilon_1}\,|\vec{r} - \vec{r}_a|\right) + \frac{i\alpha}{4\pi} \int_{-\infty}^{\infty} \frac{R^{E(H)}(h)}{g_1} \times e^{ig_1 k(y + y_a + 2b) + ihk(x - x_a)} dh$$
$$g_i = \sqrt{\varepsilon_i - h^2}, \quad i = 1,2,3, \quad \alpha^E = 1, \quad \alpha^H = \varepsilon. \quad (8)$$

In the integrands of the nonsingular terms of (8), the following factors appear:

1. Two dielectric half-spaces

$$R^{(E)} = \frac{g_1 - g_2}{g_1 + g_2}, \quad R^{(H)} = \frac{\varepsilon_2 g_1 - \varepsilon_1 g_2}{\varepsilon_2 g_1 + \varepsilon_1 g_2} \quad (9)$$

2. Grounded dielectric slab

$$R^{(E)} = \frac{ig_1 \sin(kg_2 d) + g_2 \cos(kg_2 d)}{ig_1 \sin(kg_2 d) - g_2 \cos(kg_2 d)}$$
$$R^{(H)} = \frac{ig_1 \varepsilon_2 \cos(kg_2 d) - g_2 \sin(kg_2 d)}{ig_1 \varepsilon_2 \cos(kg_2 d) + g_2 \sin(kg_2 d)} \quad (10)$$

3. Asymmetrical dielectric slab. See (11) at the bottom of the next page.

The Green's functions given by (8) correspond to the case where both the source and observation points are in the upper half-space, i.e., $y > -b$, $y_s > -b$, and satisfy the continuity conditions at the media interfaces. Further, by imposing the boundary conditions on the resonator contours, a set of four coupled homogeneous singular IEs for the unknown density functions can be obtained similarly to [21, eqs. (14)–(17)]. The aim is to determine those complex values of the parameter ka that generate nontrivial solutions of these IEs.

IV. Procedure of Analytical Regularization

The Green's functions G_1, G_ε, and G in the kernels of obtained IEs are known to have logarithmic singularities at $\vec{r} \to \vec{r}_s$. To handle the singular parts of the kernels of IEs, we use the integral operator regularization (semi-inversion) [20], [21]. Here, it is based on the analytical inversion of the frequency-dependent singular parts corresponding to the isolated (in the free-space) ring DR. We recall that the free-space scattering from a circularly layered cylinder can be solved in explicit form leading to infinite series. This is due to the fact that the functions $\{e^{imt}\}_{m=-\infty}^{\infty}$ form the set of orthogonal eigenfunctions of the integral operator with the corresponding kernel functions. Therefore, now we build a Galerkin-type MoM scheme with the aforementioned exponents as global expansion functions. Here, we expand the unknown functions as follows (the superscript $E(H)$ is again omitted):

$$\psi(\vec{r}_a) = \frac{2}{i\pi a} \sum_{m=-\infty}^{\infty} x_m e^{im\varphi} \tag{12}$$

with similar expansions in other partial domain, and handle the kernel functions and the right-hand side (RHS) functions of IEs similarly to [21]. On using some algebra and the orthogonality of exponents in the term-by-term integration, we exclude some of the unknowns and arrive at the homogeneous infinite-matrix equation for the coefficients $\tilde{X} = \{\tilde{x}_m\}_{m=-\infty}^{\infty}$, where $\tilde{x}_m = x_m J_m(k_1 a) m! 2^m (k_1 a)^{-m}$, $k_1 = k\sqrt{\varepsilon_1}$, as follows:

$$\left(I + A^{E(H)}\right) \tilde{X} = 0 \tag{13}$$

where $I = \{\delta_{mn}\}_{m,n=-\infty}^{\infty}$, $A^{E(H)} = \left\{A_{mn}^{E(H)}\right\}_{m,n=-\infty}^{\infty}$

$$A_{mn}^{E(H)} = \frac{i^{m-n} 2^{m-n} m! \Omega_{m+n}}{(k_1 a)^{m-n} n! \left(1 + iB_m^{E(H)}\right)} \tag{14}$$

$$\Omega_n^{E(H)} = -H_n^{(1)}(2kb) + \frac{2i}{\pi} \int_{-\infty}^{\infty} \frac{R^{E(H)}(h)+1}{g_1} (h - ig)^n e^{2igkb} dh. \tag{15}$$

For simplicity, if $c = 0$ (solid dielectric resonator), then

$$B_m^{E(H)} = \frac{W^{E(H)}\left\{J_m(ka\sqrt{\varepsilon_b}), Y_m(k_1 a)\right\}}{W^{E(H)}\left\{J_m(ka\sqrt{\varepsilon_b}), J_m(k_1 a)\right\}}$$
$$W^{E(H)}\{f, g\} = \alpha^{-1}\sqrt{\varepsilon_b} f' g - \sqrt{\varepsilon_1} f g' \tag{16}$$

and, if otherwise, the expressions of [21, eq. (28)] are valid.

Here, J_n and Y_n are the Bessel and Neumann functions, respectively, and the prime is for the derivative with respect to the argument. As known from [25], a free-from-error accumulation algorithm for computing the Bessel functions with complex arguments must be based on the backward-recurrence technique. However, for the Neumann functions, it must start from certain intermediate index value and continue up and down. The evaluation of the functions $\Omega_n^{H(E)}$ is one of the most time-consuming parts of the whole algorithm, since it needs a numerical integration. It should be done carefully in view of the integrand function behavior. Using in (15) wavenumbers normalized by k plays a crucial role since it brings the integration contour to the real h axis (Fig. 2) for any k.

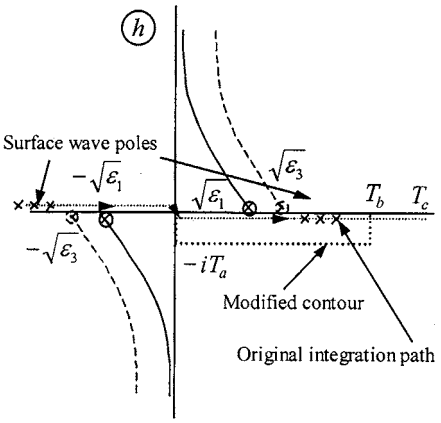

Fig. 2. Complex h plane and the contour of integration chosen for numerical evaluation of spectral integrals.

In the case of the geometries of Fig. 1(a) and (c), there are four branch points on the original integration contour, at $h = \pm\sqrt{\varepsilon_1}$ and $h = \pm\sqrt{\varepsilon_3}$. If, however, $\varepsilon_1 = \varepsilon_3$ in Fig. 1(c), then there is only one branch point at $h = \pm\sqrt{\varepsilon_1}$, and this is the case of Fig. 1(b). Besides, in the cases of Fig. 1(b) and (c), there exists a finite number $Q^{E(H)}$ of poles at $h = \pm h_p$ corresponding to the natural modes of the slab that are guided ones ($\mathrm{Im}\, h_s = 0$) if $\mathrm{Im}\, k = 0$. For these modes, one can verify that if $\mathrm{Im}\, k \neq 0$, then $\mathrm{Im}\, h_p\, \mathrm{Im}\, k > 0$.

To smooth the integrand and speed up computations, we follow the procedure frequently met in the computations of Sommerfeld's integrals. First, we convert the integrals to the ones along the positive $\mathrm{Re}\, h > 0$ semi-axis. Then, the path of integration is deformed to be composed of the four straight-line segments between the points: 1) $h = 0$; 2) $h = -iT_a$; 3) $h = T_b - iT_a$; 4) $h = T_b$; and 5) $h = T_c$, where $T_b = 1/\mathrm{Re}(kb)$, $T_b = \sqrt{\varepsilon_2} + 1$ (Fig. 2). Location of the termination point depends on the rate of the integrand decay on the last segment and can be taken as $T_c = 15/\mathrm{Re}(kb)$. Thus, the branch points are bypassed, and the contribution of the poles is accounted for automatically, provided that they lie above the deformed contour.

To determine the complex natural frequencies of the WGMs of the resonator, we search the values of the normalized frequency parameter ka that are characteristic numbers of the ma-

$$R^{(E)} = \frac{(g_1+g_2)(g_2-g_3)\exp(2ikg_2d) + (g_1-g_2)(g_2+g_3)}{(g_1-g_2)(g_2-g_3)\exp(2ikg_2d) + (g_1+g_2)(g_2+g_3)}$$
$$R^{(H)} = \frac{(\varepsilon_2 g_1 + \varepsilon_1 g_2)(\varepsilon_3 g_2 - \varepsilon_2 g_3)\exp(2ikg_2d) + (\varepsilon_2 g_1 - \varepsilon_1 g_2)(\varepsilon_3 g_2 + \varepsilon_2 g_3)}{(\varepsilon_2 g_1 - \varepsilon_1 g_2)(\varepsilon_3 g_2 - \varepsilon_2 g_3)\exp(2ikg_2d) + (\varepsilon_2 g_1 + \varepsilon_1 g_2)(\varepsilon_3 g_2 + \varepsilon_2 g_3)} \tag{11}$$

trix operator $A^{E(H)}(ka)$, i.e., the points at which the determinant of the matrix equation vanishes, as follows:

$$\det\left(I + A^{E(H)}(ka)\right) = 0. \tag{17}$$

The Fredholm second-kind nature of (13), as well as the analyticity of operators $A^{E(H)}$ in k on Ω, follows from the following estimation: $|A_{mn}| \leq \text{const}\,(a/2b)^{m+n}$. Here, $|m|$ and $|n|$ are large numbers (for details, see Appendix II). Then, the Fredholm-type theorems for operators depending on parameter [26] guarantee that the characteristic numbers of (17), i.e., the eigenvalues, form a countable set of isolated points on Ω. Due to all this, after the matrix truncation, (17) can be solved numerically, with a guaranteed convergence to the exact values of the characteristic numbers of infinite matrix. Convergence is understood here as the possibility of having computation error progressively minimized to machine precision, by taking the truncation number N greater. The proof is based on the results of [27]. The roots of (17) are found by searching in the complex domain with the Powell hybrid method [29]. Here, accuracy of computing (a) matrix elements, (b) determinant as a function of N, and (c) roots of (17) should be kept as $e_a < e_b < e_c$, respectively. Once the complex natural frequency has been determined, its Q factor can be obtained as follows:

$$Q = -\frac{\text{Re}(ka)}{2\text{Im}(ka)}. \tag{18}$$

Thus, although in practice the matrix used in (17) is truncated, the analytical regularization procedure reduces the impact of this, and the method shows guaranteed and fast convergence with increasing truncation number.

V. Numerical Results and Discussion

WGMs in an isolated DR can be classified, according to [7] and [16], as $WGE^{\pm}_{m,n}$ or $WGH^{\pm}_{m,n}$, depending on the polarization. By tradition, the notation $WGE(H)^{\pm}_{m,n}$ corresponds to the case of the transverse electric (magnetic) field being essentially tangential to the DR cross section. This implies that the field component parallel to the DR axis is of opposite nature, so that $WGE(H)$ modes correspond to the $H(E)$ polarization. In a circular-cylindrical DR, WGMs can be further characterized by two modal indexes m and n. The first index m denotes the number of azimuthal variations of the mode field and coincides with the order of the Bessel function that determines the field behavior. The second index n denotes the number of variations along the radius of DR. In an isolated DR, WGMs are double-degenerate due to the circular symmetry, which corresponds to equivalency in the $\cos(n\varphi)$ or $\sin(n\varphi)$ field dependence on the azimuth coordinate. These two possible rotating senses are denoted by superscript $\pm$.

When a DR is integrated into an optical circuit, the coupling often occurs across a gap between the DR and a waveguide [2], [19]. The width of this gap determines the coupling degree between the waveguide and resonator. The coupling may also vary if the width of the slab waveguide changes, hence contributing to variation of the radiation losses of DR. It should be noted that double-degenerate resonant frequencies of an isolated DR split when the axial symmetry of the problem is disturbed by the layered environment. Instead, one obtains two independent families of natural modes having the fields expandable in terms of $\cos(n(\varphi - \pi/2))$ or $\sin(n(\varphi - \pi/2))$, respectively, that is, symmetric or asymmetric with respect to the y axis. In our notation, the superscript $\pm$ will correspond to this sort of symmetry.

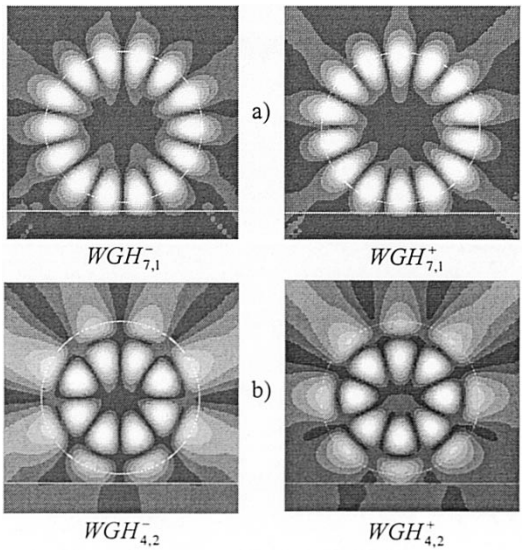

Fig. 3. Fields patterns of (a) $WGH^{\pm}_{7,1}$ and (b) $WGH^{\pm}_{4,2}$. Both are resonances of the DR located over the grounded dielectric slab waveguide with parameters $d/a = 1, \varepsilon_b = 10 + 0.001i$, and $\varepsilon_2 = 4.8$.

Field patterns of these natural modes are presented in Fig. 3(a) and (b) for the modes with one and two radial field variations, respectively. For brevity, we shall refer to the real part of a natural frequency as a resonance frequency. Note that $ka = \text{Re}(ka)(1 - i/2Q)$.

Fig. 4(a)–(f) show the resonance frequencies and Q factors of the solid circular DR modes as functions of the width of the separation gap (assumed air) for three cases of host media and for modes with one [Fig. 4(a), (c), and (e)] and two [Fig. 5(b), (d), and (f)] radial variations. It can be seen that the field interactions between the slab and WGM DR do not cause significant deviation of actual resonance frequency from that of isolated DR. However, Q factors may fall down drastically if separation gets smaller. Therefore, the coupling gap effects on the performance of the WGM DRs have to be taken into account, especially when a small gap is introduced. Larger gaps result in less perturbations of the WGM fields and, hence, less change in the natural frequencies. Furthermore, it is evident that modes with one radial field variation are much more sensitive to the presence of dielectric interfaces.

Increasing the waveguide thickness affects the DR complex natural frequencies, as shown in Fig. 5(a)–(c). Fig. 5(a) presents propagation constants of the grounded lossless dielectric-slab waveguide surface modes versus its normalized thickness d/a. It can be seen that as the value of d/a increases, new surface modes appear and resonance frequencies [Fig. 5(b)] and Q factors [Fig. 5(c)] of the DR also experience oscillations. Crosses on the graphs show the points at which new surface modes appear. Besides, decreasing the thickness of a dielectric layer to zero, we can consider a DR located over a perfect electric conductor (PEC) plane. It can be seen that the presence of the PEC

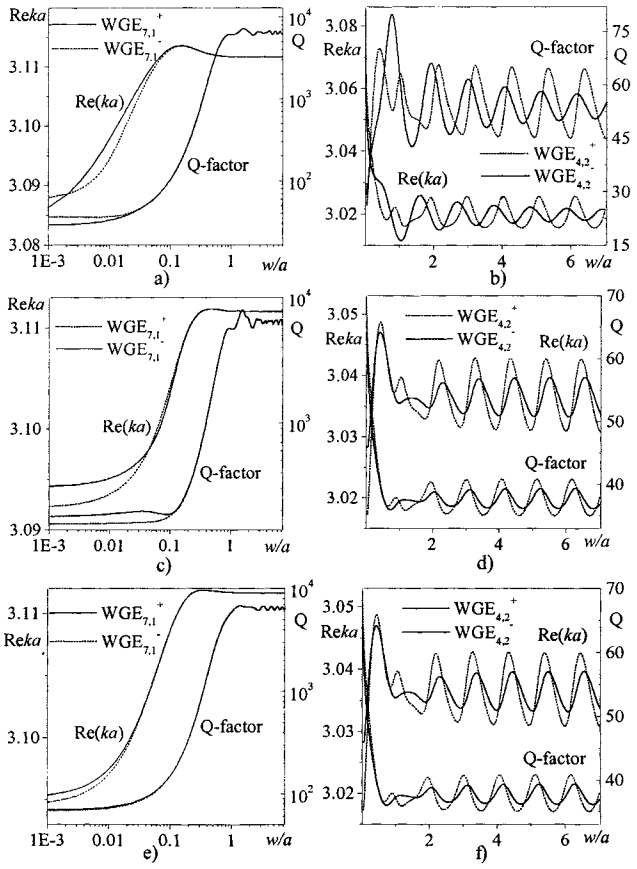

Fig. 4. Shift of the WGM resonance frequencies of a circular-cylindrical DR ($\varepsilon_b = 10 + 0.001i$) in the free half-space ($\varepsilon_1 = 1$) due to the presence of (a), (b) dielectric-dielectric interface ($\varepsilon_2 = 9$); (c), (d) grounded dielectric-slab waveguide ($d/a = 1$, $\varepsilon_2 = 4.8$); (e), (f) assymetrical dielectric waveguide ($d/a = 1, \varepsilon_2 = 6, \varepsilon_3 = 4$).

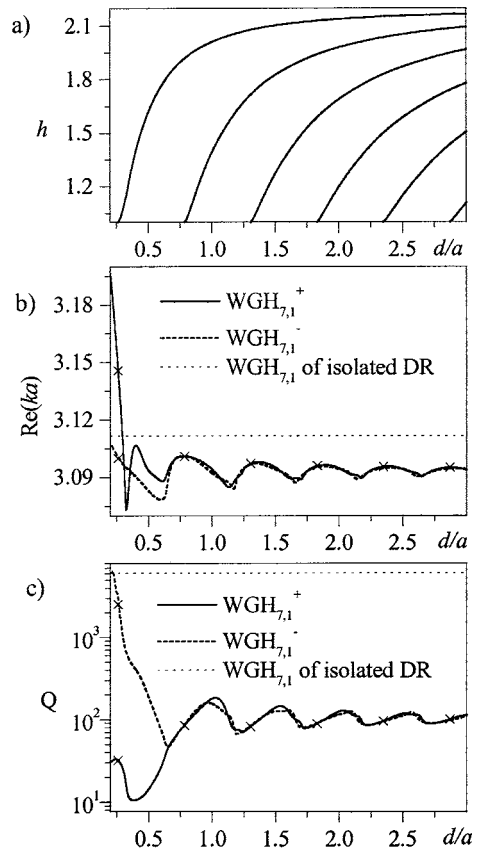

Fig. 5. Normalized propagation constants of the (a) grounded dielectric-slab eigenmodes, (b) WGM natural frequencies, and (c) Q factors of DR versus the slab thickness $w/a = 0.01, \varepsilon_b = 10 + 0.001i, \varepsilon_2 = 4.8$.

plane has a strong influence on $WG^{+}_{m,n}$ modes and almost does not affect $WG^{-}_{m,n}$ modes of the DR.

Fig. 6(a) and (b) shows the resonance frequencies and Q factors of a DR for the case of the geometry of Fig. 1(a) as functions of the lower half-space permittivity. Since the dielectric interface does not support any surface waves, no oscillation is visible, and it is seen that the Q factors of resonances are the most affected if the values of dielectric constants of the lower half-space (ε_2) and DR (ε_b) coincide. This is because here both the separation and contrast between DR and lower half-space is small, and the DR modal field leaks out with minimum reflection. Ring DRs are often used to provide a wider range free of parasitic modes. Since WGMs are characterized by a strong energy confinement within a small region between the outer rim and inner caustic, removing dielectric material from the central part of a DR does not affect the WGM field unless the inner radius of DR gets smaller than the radius of the caustic.

Fig. 7 shows the shifts in resonance frequencies and degradation of Q factors due to the change of parameter c/a. One can see that increasing the inner radius of the DR destroys resonances with several radial variations, while high-Q resonances having one radial variation can still survive in very thin rings. Here, there is a phenomenon that cannot be predicted by any approximate technique. An increase of the Q factors of the principal-family modes can be achieved at certain values of c/a, where a coincidence of the real parts of natural frequencies with those of the modes having two radial field variations occurs.

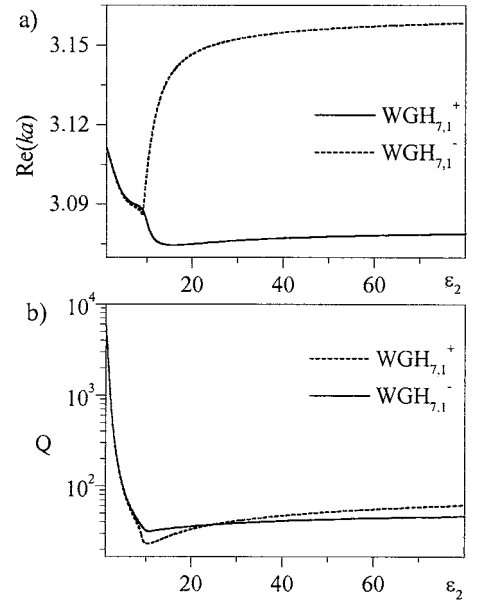

Fig. 6. (a) WGM resonance frequencies and (b) Q factors of DR over the dielectric boundary versus the permittivity of the lower half-space. $w/a = 0.001, \varepsilon_b = 10 + 0.001i, \varepsilon_1 = 1$.

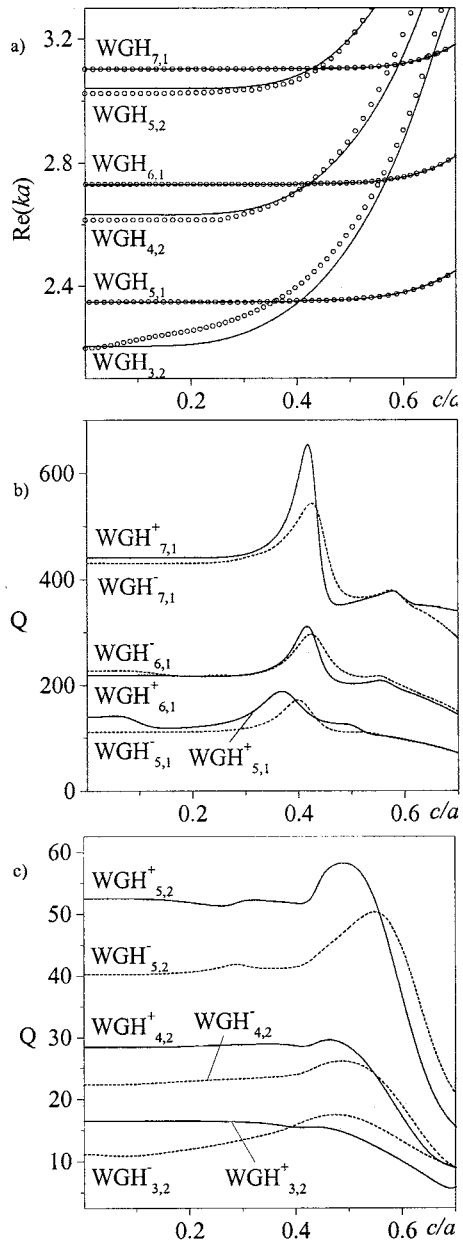

Fig. 7. Resonance frequencies and Q factors of WGMs of a ring DR located over a grounded dielectric slab versus the inner radius of the resonator. $w/a = 0.01$, $d/a = 1$, $\varepsilon_b = 10 + 0.001i$, $\varepsilon_2 = 4.8$. In (a), the solid lines are for the $(+)$ oscillations, and the circles are for the $(-)$ ones.

VI. Conclusion

A full-wave IE approach has been applied to the analysis of the natural frequencies of the WGM DRs in a layered environment. Based on this, an efficient numerical technique has been developed, and complex frequencies of the WGMs of ring DRs in several types of layered dielectric media have been calculated. Due to the analytical regularization, our solutions possess uniform numerical convergence, and no spurious eigenvalues appear. It has been shown that the frequency degeneration of the WGMs of an isolated DR is removed if the DR is immersed into a stratified medium.

Furthermore, a different dependence of the WGMs with one and two radial variations on the arrangement of host medium has been demonstrated. Thus, the method of [21] has been modified to the study of eigenvalue problems that are important in optoelectronic applications. Together with recent progress in developing a generalized method of analytical regularization (MAR) algorithm applicable to the study of 2-D DRs of arbitrary cross section [30], this forms a universal framework for accurate simulation of a wide class of DRs.

Appendix I

If a 2-D DR is placed in *free space* and excited by a known localized source with a harmonic time dependence e^{-ikct}, $\operatorname{Im} k = 0$, then the adequate condition imposed on the total-field function $U(k,\vec{r})$ at $r \to \infty$ is the Sommerfeld condition [23], [28]. The Green's function of the Helmholtz equation matched to this condition is

$$G_0(k,\vec{r},\vec{r}') = \frac{i}{4}H_0^{(1)}(k|\vec{r}-\vec{r}'|). \tag{A1}$$

The matching is understood in the sense that the following property holds:

$$\lim_{L\to\infty}\oint_L \left[U(k,\vec{r})\frac{\partial G_0(k,\vec{r},\vec{r}')}{\partial n} - G_0(k,\vec{r},\vec{r}')\frac{\partial U(k,\vec{r})}{\partial n}\right] dl = 0 \tag{A2}$$

where L is an arbitrary closed curve with outer unit normal $\vec{n}$, and U satisfies the Sommerfeld condition as well. Therefore, one can use Green's function for building the scattering-theory contour IEs, whose kernels are G_0 and its normal derivative [23], [28]. Furthermore, one can verify that no real k can be an eigenvalue of the scattering problem. It is evident that the domain of analytic continuation of $G_0(k)$ in k is the Riemann surface Λ of the function $\operatorname{Ln} k$. This is an infinite-sheet surface with the branch point at $k = 0$. Hence, the domain of analyticity of $U(k,\vec{r})$ cannot be wider than Λ. The principal sheet Λ_0 is selected by making a branch cut along the negative k axis as follows: $\Lambda_0 = \{-\pi/2 < \arg k < 3\pi/2\}$.

Reichardt has shown [24] that for the complex values of k, the following condition plays the role of analytic continuation of Sommerfeld's condition: at $r \to \infty$ (actually, for all $r > C$), the solution is expandable as a uniformly convergent series

$$U(k,\vec{r}) = \sum_{n=-\infty}^{\infty} a_n H_n^{(1)}(kr)e^{in\varphi}. \tag{A3}$$

This condition ensures that even for complex k, the property (A2) holds true. Therefore, the Fredholm second-kind IEs known in the real-k scattering analyzes [23], [28] are valid for all complex values of k as well. This enables one to use the theory of operator-valued functions to study the properties of $U(k,\vec{r})$. Here, the operator generalization of the Fredholm theory made by Steinberg [26] leads to the conclusion that $U(k,\vec{r})$ is no more than a finite-meromorphic function of k varying on Λ, i.e., it may have only a countable number of finite-multiplicity poles with the single accumulation point at

infinity. Another immediate corollary is that the residues in the simple poles are

$$\operatorname*{Res}_{k=k_s} U(k,\vec{r}) = C_s U_s(k_s,\vec{r}) \tag{A4}$$

where C_s is a constant, and each function $U_s(k,\vec{r})$ satisfies the *homogeneous* (no sources) problem with $k = k_s$ on Λ. Therefore, k_s represents the *generalized eigenvalues* of the problem—they form the spectrum of natural modes—and $U_s(k,\vec{r})$ represents the corresponding *generalized eigenfunctions*—they are the natural-mode field functions. The Poynting theorem applied to the natural-mode field and its complex conjugate leads to a conclusion, due to (A2), that, on Λ_0, the natural frequencies can be located only in the lower half-plane ($\operatorname{Im} k < 0$). It means that $U(k,\vec{r})$ is analytic (has no poles) in the upper half-plane of $\Lambda_0(\operatorname{Im} k > 0)$ and on its real axis ($\operatorname{Im} k = 0$). The convenience of the chosen definition of the principal sheet is that it leads to the symmetry of natural frequencies with respect to the imaginary k axis (verified by the direct substitution). Similarly, if k is on Λ_0 and $kr \gg 1$, then

$$H_n^{(1)}(kr) \sim \left(\frac{2}{i\pi kr}\right)^{1/2} (-i)^n e^{ikr}. \tag{A5}$$

It is easy to see that natural-mode fields display exponential damping in time and exponential growth in the r direction.

Another important corollary of the Steinberg theorems is that each natural frequency k_s is a piece-continuous function of the geometry of DR and dielectric constant. Continuity can be spoiled only if two or more natural frequencies coalesce; they can appear or disappear only at the boundary of the domain of analyticity in k, i.e., at infinity on Λ or at $k = 0$.

Suppose now that a 2-D DR is placed into a *stratified medium*. For definiteness, we shall consider the E-polarization case of a grounded slab with $\varepsilon_2 > 0$ placed in the free half-space with $\varepsilon_1 = 1$. This geometry is shown in Fig. 1(b); however, here we place the origin of coordinates at the ground plane, the source in the first medium, and the observation point in the jth one. The Green's function of the background medium with $\operatorname{Im} k = 0$ is then given by

$$\begin{aligned} G_{1j}^{\mathrm{strat}}(k,\vec{r},\vec{r}') = {} & \delta_{1j}\frac{i}{4}H_0^{(1)}(k\,|\vec{r}-\vec{r}'|) \\ & + \frac{i}{4\pi}\int_{-\infty}^{\infty}\frac{R_j(g)}{g} \\ & \times V'(gy')V(gy)e^{ikh(x-x')}dh \end{aligned} \tag{A6}$$

where $g = (1-h^2)^{1/2}$, $j = 1, 2$, and

$$\begin{aligned} V(gy) = {} & \begin{cases} \sin(kg_2d)e^{ikg(y-d)}, & y > d \\ \sin(kg_2y), & y < d \end{cases} \\ V'(y') = {} & e^{ikg(y'-d)} \\ g_2 = {} & (\varepsilon_2 - 1 + g^2)^{1/2}. \end{aligned} \tag{A7}$$

$R_1(g)$ is similar to that in (10) and can be cast into

$$\begin{aligned} R_1(g) = {} & \frac{P(g)-1}{\sin(kg_2d)} \\ P(g) = {} & \frac{2ig\sin(kg_2d)}{ig\sin(kg_2d) - g_2\cos(kg_2d)} \underset{|h|\to\infty}{\sim} \left(|h|^{-1}\right) \end{aligned} \tag{A8}$$

$$R_2(g) = \frac{2ig}{ig\sin(kg_2d) - g_2\cos(kg_2d)}. \tag{A9}$$

The first term in the RHS of (A6) is the same as in the free space, thus providing the $\operatorname{Ln} k$ branch point at $k = 0$, and the second is a Fourier (Sommerfeld) integral. Its integrand, as a function of h, varies on the two-sheet Riemann surface Γ of $g(h) = \sqrt{1-h^2}$ for every fixed k. Here, the coefficients $R_j(g)$ are meromorphic in h on Γ. If $\operatorname{Im} k = 0$, a finite number of their poles $h_p(k)$, $p = 1, 2 \ldots Q$ are real-valued on $\Gamma_0 = \{\operatorname{Im} g > 0\}$ and located between 1 and $\sqrt{\varepsilon_2}$. Each pth residue is a function of the argument $g_p(k) = \sqrt{1-h_p^2}$, as follows:

$$\operatorname*{Res}_{h=h_p} P(g) = -\frac{2ig_p^2\sin^2(kg_{2p}d)}{h_p(1-ikg_pd)}. \tag{A10}$$

Then

$$\begin{aligned} G_{1j}^{\mathrm{strat}}(k,\vec{r},\vec{r}') = {} & \frac{i\delta_{1j}}{4} \\ & \times \left[H_0^{(1)}(k\,|\vec{r}-\vec{r}'|) - H_0^{(1)}(k\,|\vec{r}-\vec{r}^*|)\right] \\ & + 2i\sum_{p=1}^{Q(k)}\frac{V(g_py')V(g_py)}{h_pN_p^2} \\ & \times \cos(kh_p\,|x-x'|) \\ & + \int_{-\infty}^{\infty} S(h)e^{ihkx}dh \end{aligned} \tag{A11}$$

where $N_p^2 = i(1-ikg_pd)/2g_p$ is a norm of the pth surface mode, $\vec{r}^* = \{x', -y'+2d\}$ corresponds to the image of the source point with respect to the plane $y = d$, and $S(h)$ is a uniformly bounded function of h on the real axis of Γ_0.

Therefore, for any real k, in addition to the logarithmic branch point at $k = 0$, the stratified-medium Green's function $G^{\mathrm{strat}}(k)$ has finite number of square-root branch points at $k = \pm k_p$, $p = 1, 2, \ldots Q$ located on the real axis of the principal sheet Λ_0 of the logarithm, where k_p is the "critical frequency" of the pth guided mode $h_p(k_p) = 1$. Hence, the full domain of analytic continuation of $G^{\mathrm{strat}}(k)$ to complex k is the Riemann surface Ω of the function $\operatorname{Ln} k + \sum_{p=1}^{Q} g_p(k)$. This is a major difference from the *closed* parallel-plate PEC waveguide Green's function, which has no logarithmic branch point but only an infinite number of simultaneous branch points and poles at $k_p = \pi p/d (|p| = 0, 1, 2 \ldots)$, where d is the plate separation. The principal ("physical") sheet is then selected as $\Omega_0 = \{-\pi/2 < \arg k < 3\pi/2,\ \operatorname{Im} g_p(k) > 0,\ p = 1, 2, \ldots\}$.

Therefore, if k is assumed in a bounded domain on Ω and $r \to \infty$, the solution of the problem about DR located in the first medium behaves as

$$U_j(k,\vec{r}) = R_j(k,\vec{r}) + W(k,\vec{r}), \quad j = 1, 2 \tag{A12}$$

$$R_1(k,\vec{r}) = \sum_{n=-\infty}^{\infty}\alpha_n H_n^{(1)}(kr)\,e^{in\varphi},\ R_2(k,\vec{r}) = 0 \tag{A13}$$

$$W(k,\vec{r}) = \sum_{p=1}^{Q}\begin{cases} \beta_p^+ V(g_py)e^{ih_pkx}, & x > 0 \\ \beta_p^- V(g_py)e^{-ih_pkx}, & x < 0 \end{cases} \tag{A14}$$

where α_n, $\beta_p^{\pm}$, and Q are constants depending on k. Expression (A12) can be considered as a "modified" Reichardt condition.

It can be shown to guarantee that the natural frequencies are located on Ω_0 only at $\mathrm{Im}\ k < 0$. The second term in (A12) contains contributions of the poles h_p as follows: $\mathrm{Im}\ h_p < 0$. These poles are the guided-mode poles previously located on the real h axis when $\mathrm{Im}\ k = 0$; they shift now to the lower h half-plane. For any fixed k, the number of these poles is finite $Q(k)$. With condition (A12), in particular, (A2) and (A3) hold true. Fortunately, the Steinberg theorems do not depend on the specific arrangement of the domain of analytic continuation in k because they are valid for k in any compact subdomain. Therefore, all the properties of the natural-frequency spectrum on Ω are principally the same as in the case of the homogeneous host medium. Modal fields here display exponential growth along $|x|$ due to the contribution of the second term in (A12). This is because for the guided modes, $\mathrm{Im}\ k < 0$ entails $\mathrm{Im}\ (kh_p) < 0$.

APPENDIX II

The well-known $n \gg |z|$ estimates, which follow from the series expansions of the cylindrical functions, are

$$J_n(z) < \frac{|z|^n}{n!2^n}, \quad H_n^{(1)}(z) < C\frac{(n-1)!2^n}{|z|^n} \tag{B1}$$

uniformly with respect to z in any bounded subdomain on Λ. Further, the Fourier coefficients of the stratified-medium Green's function can be cast into the following form:

$$\Omega_n(kb) = -H_n^{(1)}(2kb) + \int_{-\infty}^{\infty} P(g)\frac{(h-ig)^n}{g}e^{2igkb}dh \tag{B2}$$

where $g = (1-h^2)^{1/2}$ and $P(g)$ is given by (A8). Introducing the function

$$W(g) = \frac{P(g)}{g} - \sum_{p=1}^{Q} S_p(h_p)\frac{2h_p}{h^2 - h_p^2} \tag{B3}$$

where S_p is a residue of $P(g)/g$ at $h = h_p$, we bring (B2) to the form

$$\begin{aligned}\Omega_n(kb) = &- H_n^{(1)}(2kb) \\ &+ i\pi\sum_{p=1}^{Q} S_p(h_p) \\ &\times \left[(h_p - ig_p)^n + (-h_p - ig_p)^n\right]e^{2ig_pkb} \\ &+ \int_{-\infty}^{\infty} W(g)(h-ig)^n e^{2igkb}dh.\end{aligned} \tag{B4}$$

As the integrand of the last term in (B4) is bounded by $C|h|^{n-1}e^{-2|h|kb}$ for all real h, this integral is analytic in k. It is easy to verify that each $S_p(k)$ has square-root branch points associated with $k = \pm k_p$: $h_p^2(k) = 1$. Hence, it follows that $\Omega_n(k)$ is analytic on the Riemann surface Ω.

Further, as $n!$ grows more rapidly than any power function, the asymptotic large-n behavior of $\Omega_n(k)$ is the same as for the Hankel function. Eventually, on making use of the formulas (B1), one can see that

$$A_{mn} < \mathrm{Const}(k)\left(\frac{a}{2b}\right)^n \tag{B5}$$

uniformly in any bounded domain on Ω. This is enough to prove that the following property of the infinite-matrix operator A holds true:

$$\sum_{m=-\infty}^{\infty}\sum_{n=-\infty}^{\infty}|A_{mn}(k)|^2 < \infty. \tag{B6}$$

Therefore, operator equation $(I+A)X = 0$ is a homogeneous canonic Fredholm one [26] in the space of number sequences l_2. Its characteristic numbers k_s (coinciding with the natural frequencies in view of the spectral equivalency) are given by the roots of determinant equation $\mathrm{Det}(I + A(k)) = 0$. It has been shown [27] that the proposed Galerkin-type numerical scheme with an explicit Fourier-series representation for the main part of the operator converges very fast. A convergence rate of the discetization scheme is determined by the rate of decay of the matrix elements given by (B5) [31], [32]. One can see that the wider the air gap between DR and the nearest dielectric interface w, the higher the rate of convergence. However, the numerical scheme is stable and convergent even for very narrow air gaps. In addition, due to a known result of the superconvergence of the trigonometric projection methods [33], the rate of convergence of generalized eigenvalues k_s^N of the truncated $N \times N$ counterpart equation to the exact values k_s is twice higher than that of the scattering or eigenvector problem solution determined by (B5).

ACKNOWLEDGMENT

The authors thank an anonymous reviewer for helpful comments. A.I. Nosich is grateful to the University of Nottingham, Nottingham, U.K., for visiting opportunities.

REFERENCES

[1] C. Gmachl *et al.*, "High-power directional emission from microlasers with chaotic resonators," *Science*, no. 280, p. 1556, 1998.

[2] B. E. Little *et al.*, "Microring resonator channel dropping filters," *J. Lightwave Technol.*, vol. 15, pp. 998–1005, June 1997.

[3] A. Serpenguzel *et al.*, "Enhanced coupling to microsphere resonances with optical fibers," *J. Opt. Soc. Amer. B, Opt. Phys.*, vol. 14, pp. 790–795, Apr. 1997.

[4] S. C. Hill *et al.*, "Enhanced backward-directed multiphoton-excited fluorescence from dielectric microcavities," *Phys. Rev. Lett.*, vol. 85, pp. 54–57, Jan 2000.

[5] C. Vedrenne and J. Arnaud, "Whispering gallery modes of dielectric resonators," *Proc. Inst. Elect. Eng.*, pt. H, vol. 129, pp. 183–187, Apr. 1982.

[6] J. Krupka, "Computation of frequencies and intrinsic Q-factors of TE_{0mn} modes of dielectric resonators," *IEEE Trans. Microwave Theory Tech.*, vol. MTT-33, pp. 274–277, Mar. 1985.

[7] X. H. Jiao, P. Guillon, and L. A. Bermudez, "Resonant frequencies of whispering-gallery dielectric resonator modes," *Proc. Inst. Elect. Eng.*, pt. H, vol. 134, pp. 497–501, June 1987.

[8] D. Kajfez, A. W. Glisson, and J. James, "Computed modal field distribution for isolated dielectric resonators," *IEEE Trans. Microwave Theory Tech.*, vol. MTT-32, pp. 1609–1616, Dec. 1984.

[9] W. Zheng, "Computation of complex resonance frequencies of isolated composite objects," *IEEE Trans. Microwave Theory Tech.*, vol. 37, pp. 953–961, June 1989.

[10] A. Navarro and M. J. Nunez, "FDTD method coupled with FFT: a generalization to open cylindrical devices," *IEEE Trans. Microwave Theory Tech.*, vol. 42, pp. 870–874, May 1994.

[11] J. A. Pereda *et al.*, "Computation of resonant frequencies and quality factors of open dielectric resonators by a combination of FDTD and Prony's methods," *IEEE Microwave Guided Wave Lett.*, vol. 2, pp. 431–433, Nov. 1992.

[12] D. Kajfez, "Incremental frequency rule for computing the Q-factor of a shielded TE_{0mp} dielectric resonator," *IEEE Trans. Microwave Theory Tech.*, vol. MTT-32, pp. 941–943, Aug. 1984.
[13] R. K. Mongia and P. Bhartia, "Accurate conductor Q-factor of dielectric resonator placed in an MIC environment," *IEEE Trans. Microwave Theory Tech.*, vol. 41, pp. 445–449, Mar. 1993.
[14] J. Lee and Y.-S. Kim, "A new method of accurately determining resonant frequencies of cylindrical and ring dielectric resonators," *IEEE Trans. Microwave Theory Tech.*, vol. 47, pp. 706–708, Feb. 1999.
[15] S. W. Chen and K. A. Zaki, "Dielectric ring resonators loaded in waveguide and on substrate," *IEEE Trans. Microwave Theory Tech.*, vol. 39, pp. 2069–2074, Dec. 1991.
[16] D. Cros and P. Guillon, "Whispering gallery dielectric resonator modes for W-band devices," *IEEE Trans. Microwave Theory Tech.*, vol. 38, pp. 1667–1673, Nov. 1990.
[17] A. Kishk, M. R. Zunoubi, and D. Kajfez, "A numerical study of a dielectric disk antenna above grounded dielectric substrate," *IEEE Trans. Antennas Propagat.*, vol. 41, pp. 813–821, June 1993.
[18] S.-L. Lin and G. W. Hanson, "An efficient full-wave method for analysis of dielectric resonators possessing separable geometries immersed in inhomogeneous environments," *IEEE Trans. Microwave Theory Tech.*, vol. 48, pp. 84–99, Jan. 2000.
[19] S. C. Hagness, D. Rafizadeh, S. T. Ho, and A. Taflove, "FDTD microcavity simulations: Design and experimental realization of waveguide-coupled single-mode ring and whispering-gallery-mode disk resonators," *J. Lightwave Technol.*, vol. 15, pp. 2154–2165, Aug. 1997.
[20] A. I. Nosich, "The method of analytical regularization in wave-scattering and eigenvalue problems," *IEEE Antennas Propagat. Mag.*, vol. 42, pp. 34–49, Mar. 1999.
[21] S. V. Boriskina and A. I. Nosich, "Radiation and absorption losses of the whispering-gallery-mode dielectric resonators excited by a dielectric waveguide," *IEEE Trans. Microwave Theory Tech.*, vol. 47, pp. 224–231, Feb. 1999.
[22] A. I. Nosich, "Radiation conditions, limiting absorption principle, and general relations in open waveguide scattering," *J. Electromagnetic Waves Applicat.*, vol. 8, pp. 329–353, Mar. 1994.
[23] C. Muller, *Foundations of the Mathematical Theory of Electromagnetic Waves*. Berlin, Germany: Springer-Verlag, 1969, sec. 21, 23.
[24] H. Reichardt, "Ausstrachlungsbedingungen fur die wellenleichung," *Abh. Math. Seminar Univ. Hamburg*, vol. 24, pp. 41–53, 1960.
[25] C. F. du Toit, "Evaluation of some algorithms and programs for the computation of integer-order Bessel functions of the first and second kind with complex arguments," *IEEE Antennas Propagat. Mag.*, vol. 35, no. 3, pp. 19–25, June 1993.
[26] S. Steinberg, "Meromorphic families of compact operators," *Arch. Ration. Mech. Anal.*, vol. 31, no. 5, pp. 372–379, 1968.
[27] J. Saranen and L. Schroderus, "Some discrete methods for boundary integral equations on smooth closed curves," *SIAM J. Numer. Anal.*, vol. 32, no. 5, pp. 1535–1564, Oct. 1995.
[28] D. Colton and R. Kress, *Integral Equation Method in Scattering Theory*. New York: Wiley, 1983.
[29] W. H. Press, B. P. Flannery, S. A. Teukolsky, and W. T. Vetterling, *Numerical Recipes. The Art of Scientific Computing*. Cambridge, U.K.: Cambridge Univ. Press, 1986.
[30] S. V. Boriskina, T. M. Benson, P. Sewell, and A. I. Nosich, "Resonant spectra of the WGM dielectric resonators deformed from the circular geometry," in *Proc. Int. Conf. Math. Methods EM Theory (MMET* 2000)*, Kharkov, Ukraine, pp. 541–543.
[31] G. M. Vainikko and O. O. Karma, "The convergence rate of approximate methods in the eigenvalue problem when the parameter appears nonlinearly," *U.S.S.R. Comput. Math. Math. Phys.*, vol. 14, no. 6, pp. 23–39, 1974.
[32] L. M. Delves and K. O. Mead, "On the convergence rates of variational methods. I: Asymptotically diagonal systems," *Math. Comput.*, vol. 25, pp. 699–716, Oct. 1971.
[33] F. Chatelin, "The spectral approximation of linear operators with applications to the computation of eigenelements of differential and integral operators," *SIAM Rev.*, vol. 23, no. 4, pp. 495–522, Oct. 1981.

Svetlana V. Boriskina (S'96–A'99–M'01) was born in Kharkov, Ukraine, in 1973. She received the M.Sc. degree in radio physics with honors and the Ph.D. degree from Kharkov National University, Kharkov, Ukraine, in 1995 and 1999, respectively.

From 1997 to 1999, she was a Researcher in the School of Radio Physics at Kharkov National University, and from 2000 to 2001, a Royal Society/NATO Postdoctoral Fellow at the University of Nottingham, U.K. Currently, she is working as a Research Associate in the School of Electrical and Electronic Engineering, University of Nottingham. Her research interests are in integral equation methods for electromagnetic wave scattering and eigenvalue problems in layered media, with applications to microwave and optical waveguides, dielectric resonators, and antennas.

Trevor M. Benson (M'95–SM'01) was born in Sheffield, U.K., in 1958. He received the first-class honors degree in physics and the Ph.D. degree in electronic and electrical engineering from the University of Sheffield, Sheffield, U.K., in 1979 and 1982, respectively.

After spending more than six years as a Lecturer at University College Cardiff, U.K., he joined the University of Nottingham, U.K., as a Senior Lecturer in Electrical and Electronic Engineering in 1989. In 1994, he was promoted to the posts of Reader in Photonics and, in 1996, Professor of Optoelectronics. His present research interests include experimental and numerical studies of electromagnetic fields and waves, with particular emphasis on propagation in optical waveguides and lasers, silicon-based photonic circuits and electromagnetic compatibility.

Dr. Benson received the Clark Prize in Experimental Physics from the University of Sheffield in 1979.

Phillip Sewell (S'88–M'91) was born in London, U.K., in 1965. He received the B.Sc. degree in electrial and electronic engineering with first-class honors and the Ph.D. degree from the University of Bath, U.K., in 1988 and 1991, respectively.

From 1991 to 1993, he was a Science and Engineering Research Council (SERC) Postdoctoral Fellow at the University of Ancona, Italy. Since 1993, he has been a Lecturer and, from 2001, a Reader in the School of Electrical and Electronic Engineering at the University of Nottingham, U.K. His research interests include analytical and numerical modeling of electromagnetic problems, with application to optoelectronics, microwaves, and electrical machines.

Alexander I. Nosich (M'94–SM'95) was born in Kharkov, Ukraine, in 1953. He graduated from the School of Radio Physics of the Kharkov National University in 1975. He received the Ph.D. and D.Sc. degrees in radio physics from the same university in 1979 and 1990, respectively.

Since 1978, he has been on Research Staff of the Institute of Radio-Physics and Electronics (IRE) of the Ukrainian Academy of Sciences, in Kharkov, Ukraine. From 1992 to 2001, he held research fellowships and visiting professorships in Turkey, Japan, France, and Italy. Currently, he is a leading scientist in the Department of Computational Electromagnetics, IRE. His research interests include free-space and open-waveguide scattering, complex mode behavior, radar cross-section analysis, and antenna simulation.